ACS Sustainable Chemistry & Engineering

pubs.acs.org/journal/ascecg

Research Article

Tough and Strong All-Biomass Plastics from Agricultural and Forest Wastes via Constructing an Aggregate of Hydrogen-Bonding Networks

Zhenghao Xia,[#] Hongchao Lu,[#] Guangmei Xia,[#] Jinming Zhang,[*] Yan Zhou,[*] Qinyong Mi, Jinyang Li, and Jun Zhang[*]

Cite This: *ACS Sustainable Chem. Eng.* 2023, 11, 9153−9162

Read Online

ACCESS | Metrics & More | Article Recommendations | Supporting Information

ABSTRACT: The development of all-biomass materials to replace conventional plastics has been gradually becoming a focus. However, all-biomass plastics, especially those fabricated from agricultural and forestry wastes, have the obstacles of poor formability and/or low toughness. Herein, we demonstrated a facile, efficient, and easy-to-scale method to significantly improve the formability and toughness of biomass materials via constructing an aggregate of hydrogen-bonding networks, where the relatively weak hydrogen bonding could be sacrificed during stretching. After a continuous preparation process that combined a paper-making process with an *in situ* welding process, the regenerated cellulose material with a layered microstructure was spontaneously formed. The interlayer hydrogen-bonding interactions could dissipate energy during stretching. As a result, the cellulose plastics were tough and strong. The tensile strength, strain, and toughness reached 154.9 MPa, 57.7%, and 81.76 MJ/m^3, respectively, which were markedly higher than those of previous cellulose-based materials. The corresponding cellulose hydrogel exhibited an excellent strength of 9.5 MPa and a high strain of 171.4% also. During this scalable process, a 1-ethyl-3-methylimidazolium acetate (EmimAc) aqueous solution worked as a dispersant and a solvent, and a high solid content of cellulose/EmimAc (20 wt %) was used. Based on such an effective method, various agricultural and forestry wastes, including corn straw, wheat straw, grass, and wood powder, could be directly processed into high-tough all-biomass films, indicating a huge potential in ecofriendly materials, environmental protection, and bioresource utilization.

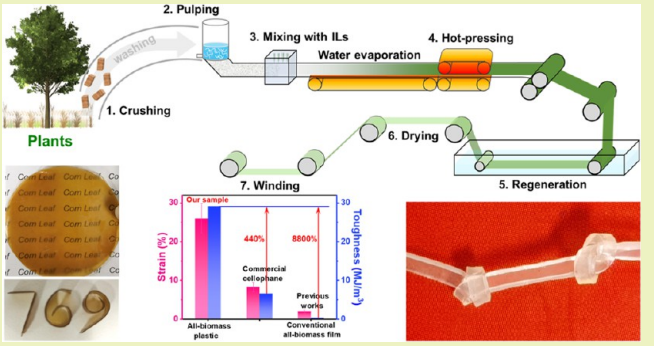

KEYWORDS: *biomass, hydrogen bonding, agricultural and forestry wastes, tough plastics, cellulose*

INTRODUCTION

Plastic products, such as plastic bags, plastic packaging, electronic devices, and medical consumables, bring great convenience to human life and have greatly promoted the development of human society.[1,2] However, due to the ultrastability of C−C bonds and the high molecular weight, the plastics are difficult to be degraded in nature, causing a series of environmental pollution problems, such as soil pollution and marine pollution.[3,4] In particular, plastic debris has scattered all over the world, and some microplastics have been found in lungs, blood, and even embryos.[5] Due to the chemical-related toxicity and size effect, microplastics can disturb organism function and further affect the health and living species.[6,7] To address the crisis, the development of various biodegradable polymers is of significant importance.[8]

Biomass, which comes from natural plants, is regarded as the most abundant bioresource in nature. It is available, renewable, tremendous, completely biodegradable, and excellently biocompatible.[9] Thus, the effective and ecofriendly utilization of natural biomass not only protects our environment but also develops new materials to replace petroleum-based plastics.[10,11] However, biomass-based materials encounter many difficulties, including poor formability and weak toughness, due to the strong bio-recalcitrance and excessive impurities.[12] For example, agricultural straw can not form stable film materials by a direct dissolution−regeneration process.[13] Although the pretreatment process and the enhancement strategy have been developed, the regenerated biomass materials from straws are still fragile.[14] In addition, even if high-quality cellulose is used as a raw material, the reported regenerated cellulose films generally exhibit poor toughness.[15] The tensile strain is less

Received: April 5, 2023
Revised: May 24, 2023
Published: June 2, 2023

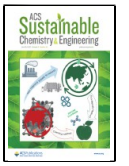

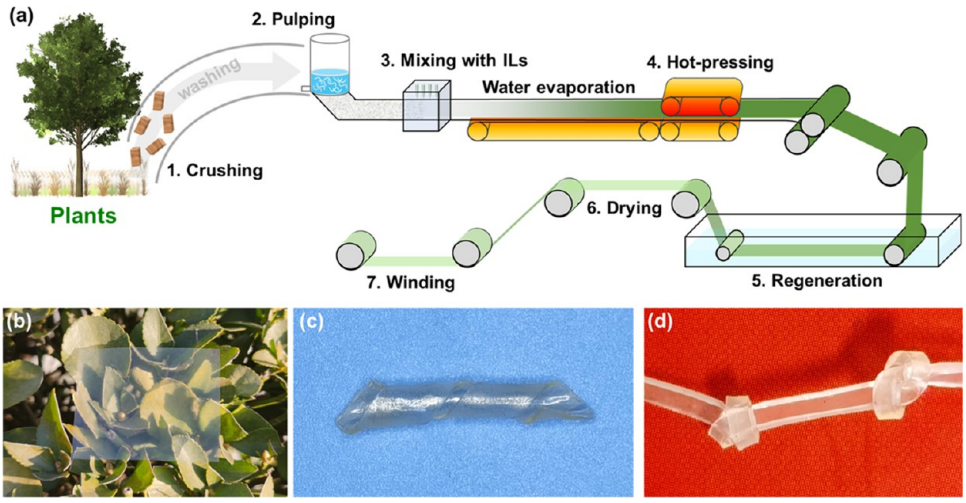

Figure 1. Schematic illustration of tough and strong biomass films. (a) Preparation process of high-tough biomass films and plastics, (b) transparent cellulose film, (c) cellulose plastic, and (d) cellulose hydrogel.

than 10%. When plenty of the plasticizer is added, the elongation at break of the cellulose film increases limitedly (<20%), while the tensile strength decreases obviously.[16] Tremendous efforts have been made to solve these problems. However, in most studies, researchers obtained high-strong biomass-based materials whose toughness was relatively weak. For example, via complete densification of the delignified wood or bamboo, superhigh-strong materials were fabricated,[17,18] but their strains were less than 2.5%. Guan et al. used cellulose nanofibers and microplatelets as the raw materials to prepare high-strong bulk materials, which had a low flexural strain of 1.5%.[19] Soykeabkaew et al. prepared all-cellulose nanocomposites by surface selective dissolution of bacterial cellulose. The obtained all-cellulose nanocomposites had a high tensile strength of 411 MPa and an extremely low strain of 4%.[20] Zhang et al. fabricated strong and tough paper with a strength of 102 MPa and a tensile strain of 18% by adding the positively charged lignosulfonate−polyamide−epichlorohydrin complex nanoparticles, which had a substantially negative effect on the biodegradability of paper.[21] Chen et al. used special hemicellulose-rich nanofibers to prepare the strong and tough paper by controlling the folding of nanofibers during drying.[22] Zhao et al. developed a double-cross-linked strategy to fabricate strong and tough cellulose hydrogels and films.[23−25] Therefore, it is appealing and challenging to fabricate tough and strong biomass materials with a novel, practical, and sustainable strategy.

Herein, we proposed a facile and effective strategy to construct high-tough and strong regenerated cellulose materials based on the formation of an aggregate of hydrogen-bonding networks, where the relatively weak hydrogen-bonding network could be sacrificed during stretching. According to this new principle, natural agricultural and forest wastes could be directly transformed into tough all-biomass materials by combining a paper-making process with an *in situ* welding process (Figure 1a).

EXPERIMENTAL SECTION

Materials. Cellulose (eucalyptus pulp) and the ionic liquid AmimCl were provided by Shandong Henglian New Materials Co., Ltd., China. Hybrid Pennisetum grass, corn straw, wheat straw, and poplar sawdust were obtained from Zhuhai Liangzhu Grass Industry Co., Ltd., China. The ionic liquid EmimAc, BmimCl, and BmimAc were purchased from the Lanzhou Institute of Chemical Physics, Chinese Academy of Sciences.

Preparation of Cellulose Hydrogels and Films. The preparation process was as shown in Figure 1a. A cellulose microfiber aqueous dispersion (3%) was fabricated by crushing the eucalyptus pulp in a home blender. A cellulose nanofiber aqueous suspension (3%) was made by treating the cellulose microfiber aqueous dispersion with a grinder (MKCA6-3, Masuko Sangyo, Japan) for 100 times at 2000 r/min. Then, EmimAc was added into the cellulose microfiber or nanofiber aqueous suspension under stirring. The solid content of cellulose/EmimAc was 10, 15, 20, 25, 28, 35, and 40%. Subsequently, the cellulose/EmimAc aqueous dispersion was poured into a mold, which was placed into an oven to remove water. The resultant cellulose/EmimAc mixture was hot-pressed at 110 °C for 5 min. After regeneration in water, the cellulose hydrogel was obtained. Finally, the regenerated cellulose plastic and film were prepared after drying the cellulose hydrogel under a vacuum at 60 °C for 12 h.

Preparation of All-Biomass Materials. The biomass powder was treated in 2% NaOH at 60 °C for 0.5 h in order to remove a small amount of hemicellulose.[13] After washing with water, the treated biomass powder aqueous dispersion (3%) was prepared. Then, EmimAc was added to get the biomass/EmimAc aqueous dispersion under stirring. The solid content of biomass/EmimAc was 20%. Subsequently, the biomass/EmimAc aqueous dispersion was poured into a mold, which was placed into an oven to remove water. The resultant biomass/EmimAc mixture was hot-pressed at 110 °C for 5 min. After regeneration in water and drying, the all-biomass material was obtained.

Characterization. The swelling and dissolution processes of cellulose in EmimAc/H_2O and AmimCl/H_2O were observed by a BX51 polarized optical microscope (Olympus, Japan). The surface and cross-sectional morphologies of the films and freeze-dried hydrogels were observed with a scanning electron microscope (JSM-6700F, JEOL, Japan) at an accelerating voltage of 5 kV. The mechanical performance of cellulose and all-biomass materials was evaluated using a universal testing machine (Instron 3365, INSTRON) with a 5 kN load cell. The crosshead speed was 2 mm/min for the films and 5 mm/min for the hydrogels. The rectangular-shaped specimens have a length of more than 50 mm and a width of 10 mm. In order to ensure accuracy and repeatability, at least five specimens were tested. Wide-angle X-ray diffractograms (WAXD) were recorded on an X-ray diffractometer (D/max-2500, Rigaku Denki, Japan) in reflection mode with Cu Kα radiation (λ = 0.154 Å) operating at 40 kV and 25 mA. The angular range (2θ) was from 5 to 40°. The scanning speed was 5°/min. Two-dimensional (2D) X-ray diffraction measurement was performed on a Xenocs Xeuss 2.0 instrument with a Cu Kα radiation source (λ = 1.54 Å) and

https://doi.org/10.1021/acssuschemeng.3c02038
ACS Sustainable Chem. Eng. 2023, 11, 9153−9162

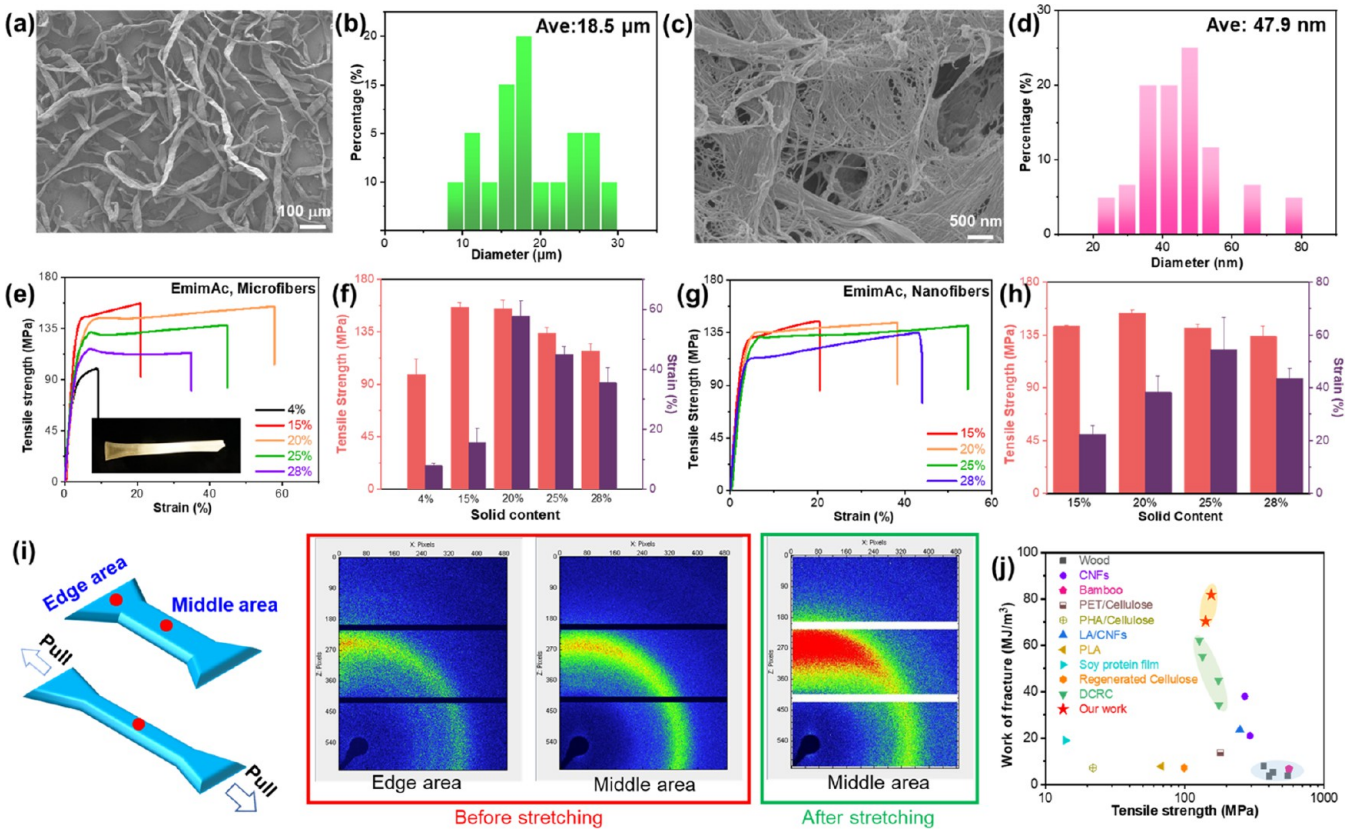

Figure 2. Mechanical properties of tough and strong cellulose films. (a) SEM image of cellulose microfibers, (b) diameter distribution of cellulose microfibers, (c) SEM image of cellulose nanofibers, (d) diameter distribution of cellulose nanofibers, (e) and (f) mechanical properties of cellulose films made by cellulose microfibers, (g) and (h) mechanical properties of cellulose films made by cellulose nanofibers, (i) WAXD patterns of cellulose films before and after stretching, and (j) toughness comparison with previous studies.[17,18,22,25,32−40]

a 2D detector (Pilatus 300 K, pixel size 172 μm) in virtual detector mode.[26] Small-angle X-ray scattering (SAXS) was recorded also on a Xenocs Xeuss 2.0 SAXS System with λ_{Cu} = 1.54 Å. The sample-to-detector distance was 2508 mm, and the calibration was performed with a silver behenate ($AgC_{22}H_{43}O_2$) standard.[27] The thermal stability test was measured by a thermogravimetric analyzer (TGA 8000, PerkinElmer) under a N_2 atmosphere from 50 to 750 °C at a heating rate of 20 °C/min. Linear viscoelastic properties of cellulose/EmimAc solutions were measured by using a TA ARES-G2 rheometer under a N_2 atmosphere with 25 mm parallel-plate geometry. The cellulose hydrogels were measured under an air atmosphere at 30 °C. An oscillatory frequency sweep was performed to measure the G' and G'' in a range of angular frequency (ω) between 10^{-4} and 10^{2} rad/s. Fourier transform infrared (FTIR) spectra were acquired in transmission mode by accumulating 64 scans at a resolution of 0.125 cm^{-1} on a Nicolet 6700 FTIR spectrometer (Thermo Fisher). The temperature was in a range of 20−240 °C. Dynamic mechanical analysis (DMA) was tested in single cantilever mode from 0 to 200 °C on a DMTA Q800 instrument (TA Instruments). The heating rate was 3 °C/min, the frequency was 1 Hz, and the amplitude was 25 μm.

RESULTS AND DISCUSSION

Preparation of High-Tough and Strong Cellulose Materials. Cellulose is the main component of biomass and is the skeleton of regenerated biomass materials to provide mechanical strength. Thus, we used cellulose as a model to develop a new processing technology for biomass.[18] Since 2002, a variety of ionic liquids (ILs) have been proven to dissolve cellulose efficiently and have been successfully used in the industrial production of regenerated cellulose materials.[28,29] Conventional ILs include 1-allyl-3-methylimidazolium chloride (AmimCl), 1-butyl-3-methylimidazolium chloride (BmimCl), 1-butyl-3-methylimidazolium acetate (BmimAc), and 1-ethyl-3-methylimidazolium acetate (EmimAc).[30] Currently, the dissolution of cellulose in ILs is realized by a strong stirring strategy at a high temperature either in the laboratory or during the industrial process. However, the solid content of the cellulose/ILs solution is difficultly higher than 10% in this strategy due to the ultrahigh viscosity. Moreover, the conventional film-formation technologies are not applicable to the biomass solution with a high viscosity and a high impurity content. Except for cellulose, natural biomass has many kinds of components, such as lignin, hemicellulose, and inorganic matter. Thus, we developed a new dissolution−regeneration strategy for processing cellulose and biomass (Figure 1a). By combining a paper-making process with an *in situ* dissolution process, cellulose or biomass powder was directly converted into tough and strong hydrogels, films, or plastics (Figure 1b−d). The new preparation process includes 7 steps: (1) crushing biomass, (2) dispersing biomass powder into ILs/H_2O, (3) spreading the biomass/ILs/H_2O mixture and evaporating water, (4) hot-pressing, (5) regeneration in water, (6) drying, and (7) winding (Figure 1a). Different from the conventional dissolution−regeneration process, the film-formation step in the new preparation process is easily achieved and is immune to the concentration and impurities, solving the obstacle of the high viscosity and the high impurity content in the biomass solution. Because the biomass/ILs/H_2O suspension with a low viscosity is spread out first, then the biomass is dissolved *in situ* by removing water. In addition,

https://doi.org/10.1021/acssuschemeng.3c02038
ACS Sustainable Chem. Eng. 2023, 11, 9153−9162

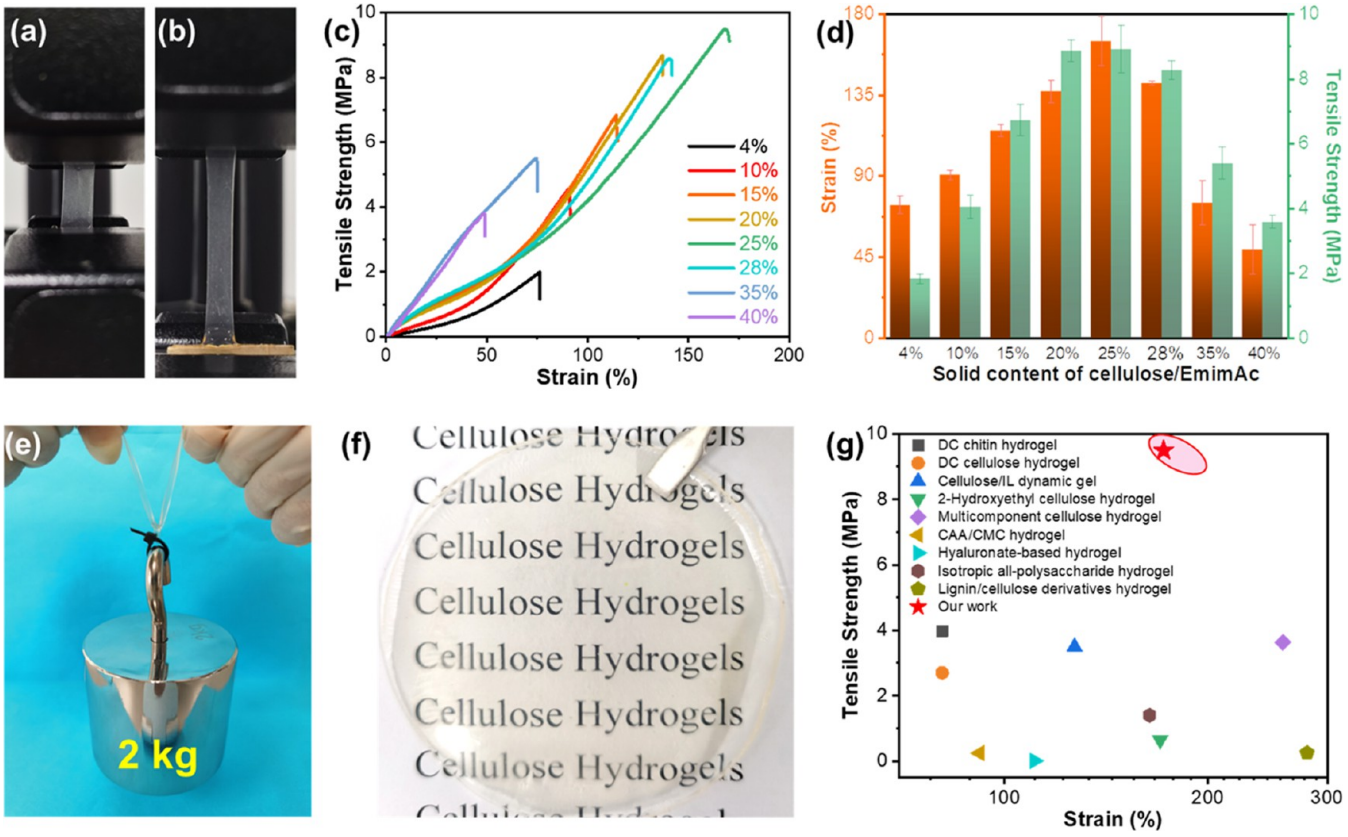

Figure 3. Tough and strong cellulose hydrogels. (a) and (b) Photographs of the stretching process of the tough cellulose hydrogel, (c) and (d) mechanical properties of cellulose hydrogels made by using cellulose nanofibers/EmimAc with different solid contents, (e) and (f) photographs of the cellulose hydrogel made by using cellulose nanofibers/EmimAc with a solid content of 25%, and (g) toughness comparison with polysaccharide-based hydrogels in previous studies.[23,45−52]

because the preparation process is stirring-free, the biomass solution with a high concentration is easily fabricated.

In order to realize the above preparation process, there are two keys: the dispersion state and the undisturbed dissolution of biomass powder. Water is a good swelling solvent of biomass. Moreover, it can remarkedly decrease the viscosity of ILs, which is beneficial to the diffusion of the solvent into the biomass, especially the high solid content conditions. Therefore, ILs/H_2O was used as a dispersant to disperse the biomass powder. In addition, the dissolving capability of ILs under the undisturbed state is of significant importance. The undisturbed dissolving capability of ILs follows the order EmimAc ≈ BmimAc > AmimCl > BmimCl (Figure S1). The ILs with an acetate anion (Ac^-) can quickly dissolve cellulose in 1 min. During the practical production process, owing to the strong interactions between ILs and water, it is hard to realize complete dehydration, which means the undisturbed dissolving capability of the ILs/water mixed solvent is essential (Figure S2). The EmimAc/H_2O and BmimAc/H_2O systems containing 5% H_2O can dissolve cellulose within 5 min. In contrast, cellulose is only swollen rather than soluble in AmimCl/H_2O and BmimCl/H_2O systems. Comparing these four ILs, EmimAc/H_2O was chosen as a dispersant and a solvent to fabricate biomass materials.

Based on the above preparation process, high-tough and strong regenerated cellulose materials were successfully prepared by using wood pulp and EmimAc/H_2O (Figure 1b−d). The wood pulp was dispersed with water to obtain a cellulose microfiber aqueous dispersion by using a home blender for 5 min (Figure S3a). The average diameter of fibers was 18.5 μm (Figure 2a,b). Subsequently, the cellulose microfiber aqueous dispersion was crushed by a grinder to obtain a cellulose nanofiber aqueous dispersion (Figure S3b). The average diameter of nanofibers was 47.9 nm (Figure 2c,d). EmimAc was added to the cellulose microfiber aqueous dispersion and the nanofiber aqueous dispersion, respectively. Then, the water was evaporated; meanwhile, the cellulose/EmimAc/H_2O mixture was hot-pressed to promote the dissolution of cellulose. Subsequently, after regeneration of cellulose in water, cellulose hydrogels were obtained (Figure 1d). Finally, regenerated cellulose materials were received by a heat drying process (Figure 1b,c). When cellulose microfibers were used as the raw materials and the solid content of cellulose/EmimAc reached 20%, the regenerated cellulose film was high-tough and strong. Its tensile strength reached 154.9 MPa, and the tensile strain was 57.7% (Figure 2e,f, and Table S1), which is much higher than the tensile strain (<10%) of the regenerated cellulose film prepared by a common dissolution−regeneration process.[31] With the further increase of the solid content of cellulose/EmimAc, the tensile strength and strain of the regenerated cellulose film decreased simultaneously. For example, the regenerated cellulose film exhibited a tensile strength of 118.6 MPa and a tensile strain of 35.5% when the solid content of cellulose/EmimAc was 28%. A similar phenomenon appeared when using cellulose nanofibers as raw materials. When cellulose nanofibers were used as the raw materials and the solid content of cellulose/EmimAc reached 25%, the high-tough and strong cellulose film was obtained and

https://doi.org/10.1021/acssuschemeng.3c02038
ACS Sustainable Chem. Eng. 2023, 11, 9153−9162

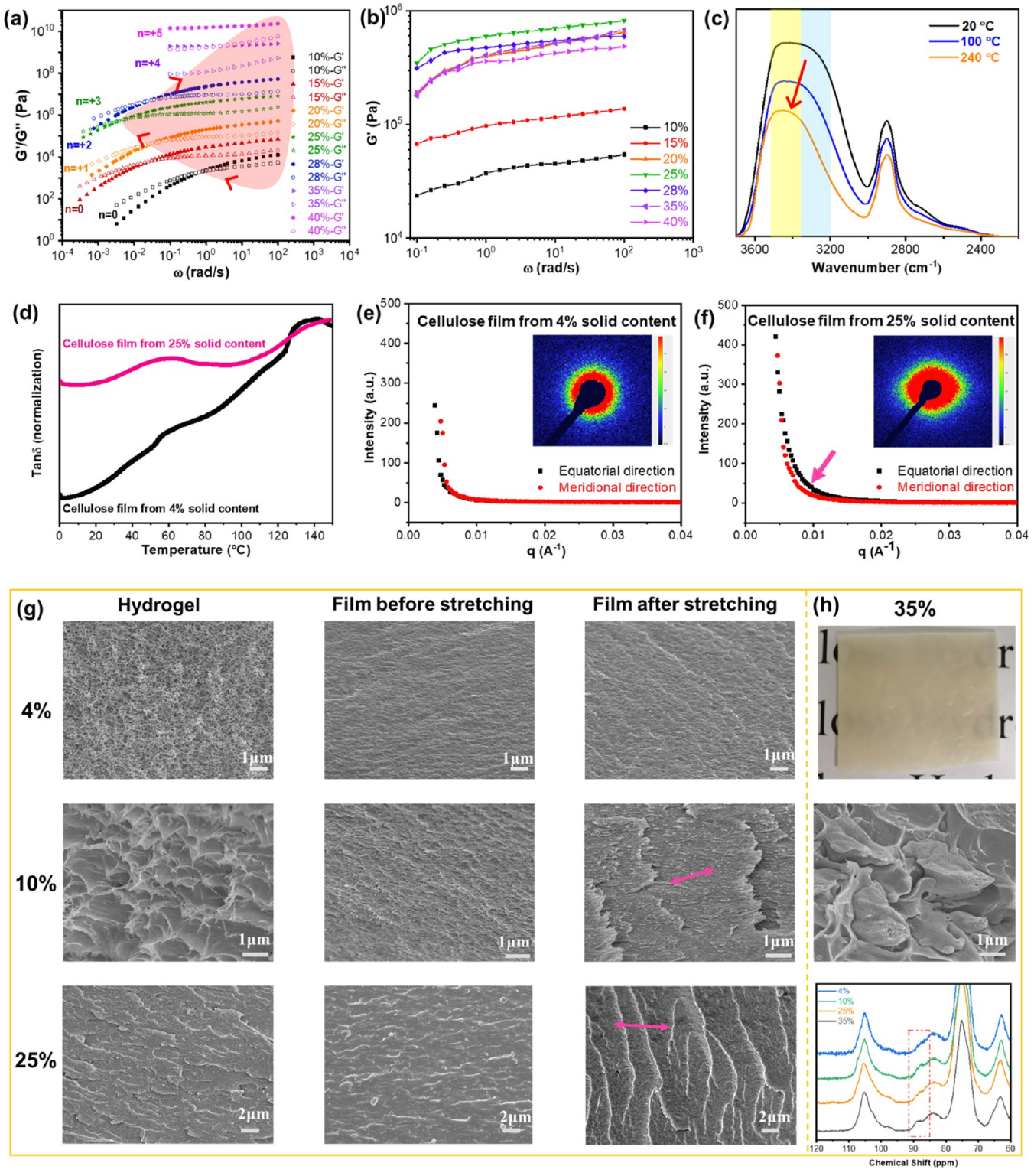

Figure 4. Mechanism of high-tough cellulose materials. (a) and (b) Rheological properties of cellulose/EmimAc solutions and regenerated cellulose hydrogels with different solid contents; (c) variable temperature FTIR spectra of cellulose films made by using cellulose nanofibers/EmimAc with a solid content of 25%; (d) DMA curves of cellulose films made by using cellulose nanofibers/EmimAc with a solid content of 25 or 4%; (e) and (f) SAXS patterns of cellulose films after stretching; (g) SEM images of cellulose hydrogels and films before and after stretching; and (h) optical image, SEM image, and solid-NMR spectra of cellulose materials made by using cellulose nanofibers/EmimAc with a solid content of 35%.

exhibited a tensile strength of 141.9 MPa and a tensile strain of 54.4% (Figure 2g,h, and Table S2). Before a stretching test, the cellulose film is homogeneous and nonoriented (Figure 2i). After a stretching test, the cellulose film exhibits an obvious orientation along the stretching direction (Figure 2i), indicating that the cellulose film has high toughness. The fracture location of the cellulose film has an obvious whitening phenomenon (Figure 2e), which is evidence of high toughness

https://doi.org/10.1021/acssuschemeng.3c02038
ACS Sustainable Chem. Eng. 2023, 11, 9153−9162

also. We also used AmimCl/H_2O as a dispersant and a solvent. The as-prepared cellulose films exhibit reduced strength and toughness than those obtained from the EmimAc/H_2O system (Figure S4) because AmimCl has a slower dissolution rate to cellulose than EmimAc under the undisturbed dissolution state and/or the presence of water. An obvious peak of a cellulose I crystal in the regenerated cellulose film confirms that the cellulose is partially dissolved in AmimCl (Figure S5). When cellulose nanofibers were used as raw materials and the solid content of cellulose/AmimCl reached 20%, the cellulose film exhibits a tensile strength of 98.5 MPa and a tensile strain of 35.0%, which is much higher than the cellulose film prepared by a conventional dissolution−regeneration process. In summary, we easily prepared high-tough and strong cellulose materials based on the above new strategy. In particular, the resultant cellulose materials have an extremely high toughness of 81.76 MJ/m^3, which is much higher than the reported toughness of cellulose-based and biomass-based materials (Figure 2j and Table S3).

High-Tough and Strong Cellulose Hydrogels. Hydrogels have attracted extensive attention due to their huge potential in wound dressings,[41] tissue engineering,[42] intelligent wear,[43] soft robots,[44] and other fields. It is attractive and challenging to fabricate high-tough and high-strong hydrogels.[45] Since the cellulose plastics prepared by the above process exhibit high toughness and high strength, the corresponding cellulose hydrogels should exhibit high mechanical properties also. The experiment results prove our conjecture. When cellulose nanofibers were used as raw materials and the solid content of cellulose/EmimAc reached 25%, the cellulose hydrogel exhibited a high tensile strength of 8.9 MPa and a high tensile strain of 165.0%, which is much higher than conventional cellulose hydrogels (Figure 3 and Table S4). The high-tough, colorless, and transparent cellulose hydrogel is not broken, even if it is stretched and recovered many times under a weight of 2 kg, indicating an excellent mechanical property (Figure 3e,f, and Video S1). With the further increase in the solid content in cellulose/EmimAc, cellulose could not be completely dissolved, resulting in a heterogeneous hydrogel with poor mechanical properties. When the solid content of cellulose/EmimAc increased to 35%, the cellulose hydrogel had a relatively low tensile strength of 5.4 MPa and a strain of 75.0%. When cellulose microfibers were used as raw materials, the cellulose hydrogel exhibited better mechanical properties. When the solid content of cellulose/EmimAc was 20%, the resultant cellulose hydrogel exhibited a high tensile strength of 9.5 MPa and a strain of 171.4% (Figure S6 and Table S5). In order to compare with the hydrogel reported in the literature, we prepared a cellulose hydrogel with a thickness of 1 mm, whose tensile strain increased to 208.8% (Figure S7). Obviously, the strength and toughness of our cellulose hydrogel are much higher than those of the polysaccharide-based hydrogels prepared by conventional methods (Figure 3g and Table S6). These phenomena indicate that the microstructure of high-tough and strong cellulose materials has been formed during the cellulose regeneration process.

Mechanism of High-Tough Cellulose Materials. A rheological test can reflect the microstructure of a polymer solution. As the solid content of cellulose nanofibers increases, the intersection point of the storage modulus (G') and the loss modulus (G'') shifts to a low frequency in a cellulose/EmimAc solution (Figure 4a), indicating that the degree of entanglement increases, and thus, an elastic response becomes dominant. The cellulose/EmimAc solution with a solid content of 25% has the lowest angular frequency at the intersection point of G' and G'' (Figure 4a). Moreover, the corresponding cellulose hydrogel has the highest value of G' (Figure 4b). The above phenomena indicate that there is the strongest entanglement network in a 25% cellulose/EmimAc solution and the corresponding cellulose hydrogel. After drying, the cellulose film was obtained. It is amorphous (Figure S8) and has high thermal stability (Figure S9). In the FTIR spectrum, a cellulose film made by using a 25% cellulose/EmimAc solution has an ultrawide peak of hydroxyl stretching vibration at 3000−3600 cm^{-1} (Figure 4c). As the temperature increases from room temperature to 240 °C, the partial hydroxyl peak disappears (Figure 4c), which means some weak hydrogen-bonding interactions are broken. DMA results show that there is only one peak of tan δ at 130 °C in the cellulose film made by using cellulose/EmimAc with a solid content of 4%, while there are two peaks of tan δ at 140 and 60 °C in the cellulose film made by using cellulose/EmimAc with a solid content of 25% (Figure 4d). Hence, the high-tough cellulose film has two kinds of hydrogen-bonding interactions, one of which is the traditional strong hydrogen-bonding interactions and the other is the new relatively weak hydrogen-bonding interactions. The weak hydrogen-bonding interactions can be sacrificed to dissipate energy once meeting an external force. As a result, the cellulose films and hydrogels made by using a high solid content of cellulose/ILs exhibit high toughness and strength.

Since the high-tough structure has been formed in cellulose hydrogels, we observed the microstructure of cellulose hydrogels that were treated by a freeze-drying process. It can be found that the cellulose hydrogel obtained by a conventional method has a porous network structure (Figure S10). When the cellulose hydrogel was prepared by using the new processing strategy and the cellulose nanofibers/EmimAc with a solid content of 4%, the cellulose hydrogel also has a porous network structure containing abundant nanofibers (Figure 4g), indicating there is a whole hydrogen-bonding network. As the solid content of cellulose increases to 10%, the obtained cellulose hydrogel shows a layered structure, indicating there are two kinds of hydrogen-bonding interactions, interlayer and intralayer hydrogen-bonding interactions. As the solid content of cellulose further increases, the cellulose layers overlap to form a dense layered interlaced structure due to the steric effect, such as the cellulose hydrogel made by using the cellulose nanofibers/EmimAc with a solid content of 25%. During the heat drying process of the cellulose hydrogel made by using the cellulose nanofibers/EmimAc with a solid content of 4%, cellulose nanofibers aggregate together, and a compact network forms. As a result, the corresponding cellulose film has a flat and dense structure (Figure 4g). During the stretching process, the nanofiber network is broken to exhibit a flat cross section. SAXS patterns show that the scattering intensities in both horizontal and vertical directions are almost the same after stretching (Figure 4e), which proves a brittle fracture during the tensile stretching process. During the heat drying process of the cellulose hydrogel made by using the cellulose nanofibers/EmimAc with a solid content of 10 and 25%, the layered structure of cellulose hydrogels is retained in the resultant cellulose films. During the stretching process, the layers slide obviously to dissipate energy because the weak interlayer hydrogen-bonding interactions are easily broken (Figure 4g). So, the corresponding cellulose materials exhibit a

https://doi.org/10.1021/acssuschemeng.3c02038
ACS Sustainable Chem. Eng. 2023, 11, 9153−9162

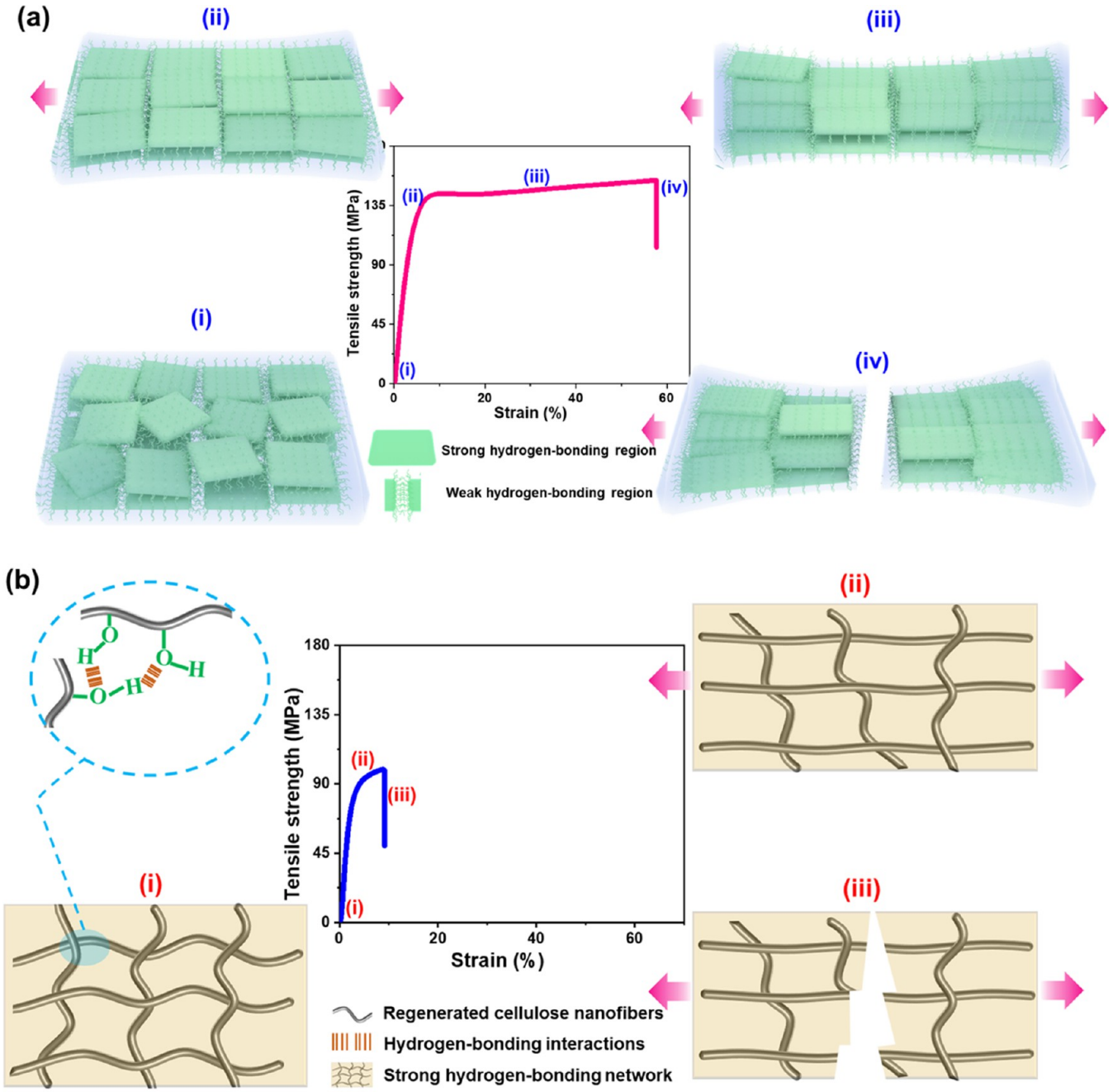

Figure 5. Mechanism schematic of high-tough cellulose materials. (a) Schematic of the fracture process of tough cellulose materials and (b) schematic of the fracture process of conventional regenerated cellulose materials.

high toughness, especially the cellulose materials with a layered interlaced structure. SAXS patterns reveal that the scattering intensity in the tensile direction increases dramatically (Figure 4f), indicating that plastic deformation occurs along the stretching direction. Combined with WAXD results (Figure 2i), it is clear that the high toughness of cellulose materials originates from the sliding and orientation of the layered structure.[53] When the solid content of cellulose nanofibers/EmimAc is higher than 25%, cellulose nanofibers could not be totally dissolved (Figure S8). A phase separation structure consisting of the regenerated cellulose and insoluble cellulose forms, resulting in a decrease in the transparency and mechanical properties of cellulose hydrogels (Figure 4h). In sum, cellulose materials with a layered interlaced structure exhibit optimal toughness and strength because the sliding of cellulose layers can effectively dissipate energy.

Based on the above results, the high-tough and strong cellulose materials originate from the layered interlaced microstructure with an aggregation of hydrogen-bonding networks (Figure 5a), which contains two kinds of hydrogen-bonding interactions, intralayer and interlayer hydrogen-bonding interactions. The strong intralayer hydrogen-bonding interactions endow the cellulose materials with high strength. The weak interlayer hydrogen-bonding interactions are sacrificed to dissipate energy, so the cellulose materials have high toughness, and the sliding of cellulose layers is observed. In contrast, the cellulose materials exhibit a whole network consisting of abundant nanofibers by using a conventional

https://doi.org/10.1021/acssuschemeng.3c02038
ACS Sustainable Chem. Eng. 2023, 11, 9153−9162

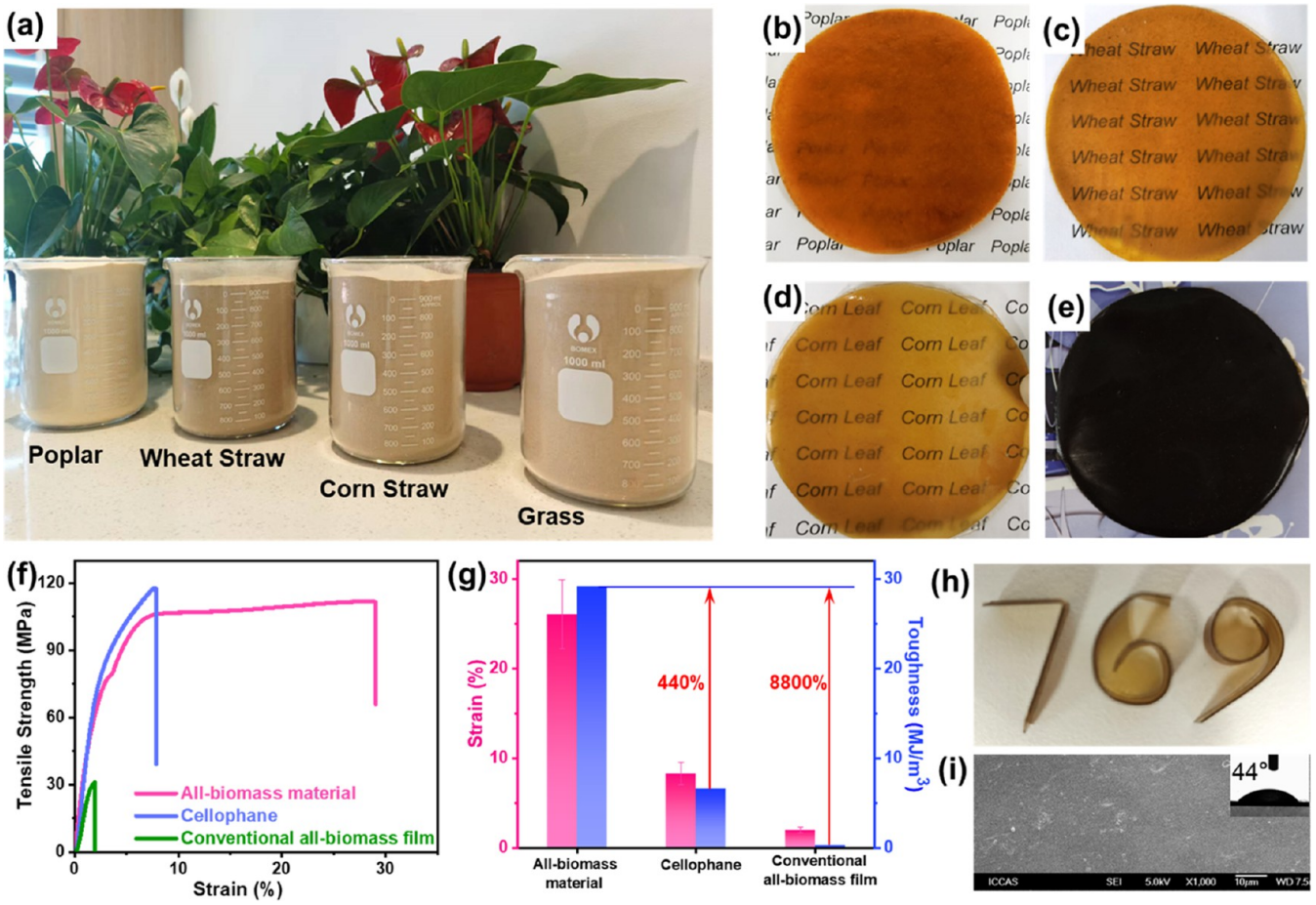

Figure 6. Tough all-biomass materials. (a) Optical images of four kinds of biomass powders; (b) optical image of all-biomass material from poplar sawdust; (c) optical image of all-biomass material from wheat straw; (d) optical image of all-biomass material from corn straw; (e) optical images of all-biomass material from grass; (f) and (g) mechanical property comparison between the all-biomass material, cellophane, and the conventional all-biomass film; and (h) and (i) optical image, the water contact angle, and the SEM image of all-biomass materials from poplar.

dissolution−regeneration process (Figure 5b). During the stretching process, curly cellulose nanofibers become straight, which dissipates energy limitedly. Thus, the conventional regenerated cellulose materials have a low toughness, for example, the tensile strain of cellulose films is below 10%. Our new processing strategy combines a paper-making step with an *in situ* dissolution step. During the paper-making step, cellulose powders spontaneously form a heterogeneous layered structure (Figure S11). The subsequent dissolution process can retain this structure because the high viscosity limits the movement of cellulose chains. Finally, the heterogeneous layered structure is retained in the regenerated cellulose hydrogels during the regeneration process. Thus, the final regenerated cellulose materials exhibit a layered structure or a layered interlaced structure, which can dissipate energy via the sliding of cellulose layers.

Tough All-Biomass Materials. Based on the above principle and strategy, we processed the common forestry and agricultural wastes, such as poplar sawdust, wheat straw, corn straw, and grass (Figure 6a). The forestry and agricultural wastes were crushed and passed through 100 mesh screens. Then, the biomass powders were treated with 2% NaOH at 60 °C for 0.5 h to remove a small amount of lignin and hemicellulose (Table S7) in order to weaken the biomass recalcitrance.[13] The treated forestry and agricultural wastes kept their original micromorphology (Figure S12). The solid content of biomass/EmimAc was controlled at 20% for processing. All four raw materials could be directly processed into the all-biomass materials (Figure 6b−e). Due to the retention of a large amount of lignin, hemicellulose, and inorganic substances, the all-biomass materials are colored and semitransparent. In FTIR spectra, the C=C peak at 1502 cm^{-1}, the C=O peak at 1736 cm^{-1}, and the Si−O peak at 798 cm^{-1} prove the existence of lignin, hemicellulose, and inorganic substances (Figure S13). More importantly, all-biomass materials exhibit outstanding mechanical properties. Taking poplar sawdust as an example, the tensile strength, strain, and toughness of all-biomass materials are 107.4 MPa, 26.1%, and 29.1 MJ/m^3, respectively (Figure 6f,g). Its tensile strain and toughness are much better than commercial cellophane, which is prepared by using high-quality cellulose and contains 10−15% plasticizer. Compared with an all-biomass film prepared by a conventional dissolution−regeneration process, the tensile strength increases by 230%; meanwhile, the tensile strain increases by 1200% (Figure 6f and Table S8). The obtained all-biomass materials can be bent directly, owing to good toughness (Figure 6h). In addition, because a large amount of lignin was retained, the obtained all-biomass materials showed reduced hydrophilicity and water resistance.

https://doi.org/10.1021/acssuschemeng.3c02038
ACS Sustainable Chem. Eng. 2023, 11, 9153−9162

CONCLUSIONS

In this work, we found a new principle and demonstrated a practical strategy to fabricate high-tough all-biomass materials via constructing an aggregate of hydrogen-bonding networks. We used a high solid content of cellulose/EmimAc (10−40 wt %) as a model and then combined a paper-making process with an *in situ* welding process. The regenerated cellulose material spontaneously formed a layered microstructure. The interlayer hydrogen-bonding interactions could be sacrificed during stretching. As a result, tough and strong cellulose films or plastics were obtained. When the solid content of cellulose/EmimAc was 20 wt %, the corresponding cellulose film exhibited an ultrahigh tensile strain of 57.7% and an excellent toughness of 81.76 MJ/m^3. The corresponding cellulose hydrogel exhibited an excellent strength of 9.5 MPa and a high tensile strain of 171.4% also. Such a facile and easy-to-scale strategy could be used to directly process various agricultural and forestry wastes, including corn straw, wheat straw, grass, and wood powder. The all-biomass high-tough films with a high tensile strength of 107.4 MPa and a high tensile strain of 26.1% were fabricated, indicating a huge potential in ecofriendly materials, environmental protection, and bioresource utilization.

ASSOCIATED CONTENT

Supporting Information

The Supporting Information is available free of charge at https://pubs.acs.org/doi/10.1021/acssuschemeng.3c02038.

Photographs, mechanical properties, XRD patterns, TGA curves, SEM images, chemical composition, and FTIR spectra (PDF)

Mechanical property of cellulose hydrogel (MP4)

AUTHOR INFORMATION

Corresponding Authors

Jinming Zhang − *CAS Key Laboratory of Engineering Plastics, Institute of Chemistry, Chinese Academy of Sciences (CAS), Beijing 100190, China;* orcid.org/0000-0003-3404-4506; Email: zhjm@iccas.ac.cn

Yan Zhou − *National Institute of Metrology, Beijing 100029, China*; Email: zhouyan123@iccas.ac.cn

Jun Zhang − *CAS Key Laboratory of Engineering Plastics, Institute of Chemistry, Chinese Academy of Sciences (CAS), Beijing 100190, China; University of Chinese Academy of Sciences, Beijing 100049, China;* orcid.org/0000-0003-4824-092X; Email: jzhang@iccas.ac.cn

Authors

Zhenghao Xia − *CAS Key Laboratory of Engineering Plastics, Institute of Chemistry, Chinese Academy of Sciences (CAS), Beijing 100190, China; University of Chinese Academy of Sciences, Beijing 100049, China*

Hongchao Lu − *SINOPEC Beijing Research Institute of Chemical Industry, Beijing 100013, China*

Guangmei Xia − *Key Laboratory of Pulp and Paper Science & Technology of Ministry of Education, Qilu University of Technology (Shandong Academy of Sciences), Jinan 250353 Shandong, China*

Qinyong Mi − *CAS Key Laboratory of Engineering Plastics, Institute of Chemistry, Chinese Academy of Sciences (CAS), Beijing 100190, China*

Jinyang Li − *CAS Key Laboratory of Engineering Plastics, Institute of Chemistry, Chinese Academy of Sciences (CAS), Beijing 100190, China*

Complete contact information is available at: https://pubs.acs.org/10.1021/acssuschemeng.3c02038

Author Contributions

#Z.X., H.L., and G.X. contributed equally to this work.

Notes

The authors declare no competing financial interest.

ACKNOWLEDGMENTS

This work was supported by the National Natural Science Foundation of China (Nos. 52173292 and U2004211), and the Youth Innovation Promotion Association CAS (2018040).

REFERENCES

(1) Wan, Y.-J.; Li, G.; Yao, Y.-M.; Zeng, X.-L.; Zhu, P.-L.; Sun, R. Recent advances in polymer-based electronic packaging materials. *Compos. Commun.* **2020**, *19*, 154−167.

(2) Shrivastava, S.; Trung, T. Q.; Lee, N. E. Recent progress, challenges, and prospects of fully integrated mobile and wearable point-of-care testing systems for self-testing. *Chem. Soc. Rev.* **2020**, *49*, 1812−1866.

(3) Chen, X.; Yan, N. A brief overview of renewable plastics. *Mater. Today Sustainability* **2020**, *7*−*8*, 7−8.

(4) Lebreton, L. C. M.; van der Zwet, J.; Damsteeg, J. W.; Slat, B.; Andrady, A.; Reisser, J. River plastic emissions to the world's oceans. *Nat. Commun.* **2017**, *8*, No. 15611.

(5) Paulsen, F. L.; Nielsen, M. B.; Shashoua, Y.; Syberg, K.; Hansen, S. F. Early warning signs applied to plastic. *Nat. Rev. Mater.* **2022**, *7*, 68−70.

(6) MacLeod, M.; Arp, H. P. H.; Tekman, M. B.; Jahnke, A. The global threat from plastic pollution. *Science* **2021**, *373*, 61−65.

(7) Bhatt, P.; Pathak, V. M.; Bagheri, A. R.; Bilal, M. Microplastic contaminants in the aqueous environment, fate, toxicity consequences, and remediation strategies. *Environ. Res.* **2021**, *200*, No. 111762.

(8) Xia, Q.; Chen, C.; Yao, Y.; Li, J.; He, S.; Zhou, Y.; Li, T.; Pan, X.; Yao, Y.; Hu, L. A strong, biodegradable and recyclable lignocellulosic bioplastic. *Nat. Sustainability* **2021**, *4*, 627−635.

(9) Ates, B.; Koytepe, S.; Ulu, A.; Gurses, C.; Thakur, V. K. Chemistry, Structures, and Advanced Applications of Nanocomposites from Biorenewable Resources. *Chem. Rev.* **2020**, *120*, 9304−9362.

(10) Cywar, R. M.; Rorrer, N. A.; Hoyt, C. B.; Beckham, G. T.; Chen, E. Y. X. Bio-based polymers with performance-advantaged properties. *Nat. Rev. Mater.* **2022**, *7*, 83−103.

(11) Haider, T. P.; Volker, C.; Kramm, J.; Landfester, K.; Wurm, F. R. Plastics of the Future? The Impact of Biodegradable Polymers on the Environment and on Society. *Angew. Chem., Int. Ed.* **2019**, *58*, 50−62.

(12) Himmel, M. E.; Ding, S.-Y.; Johnson, D. K.; Adney, W. S.; Nimlos, M. R.; Brady, J. W.; Foust, T. D. Biomass Recalcitrance: Engineering Plants and Enzymes for Biofuels Production. *Science* **2007**, *315*, 804−807.

(13) Xia, Z.; Li, J.; Lu, H.; Zhang, J.; Mi, Q.; Wu, J.; Zheng, X.; Zhang, J. Natural grass to all-biomass biodegradable tape and superior oil-water separation fabric. *Resour., Conserv. Recycl.* **2022**, *182*, No. 106320.

(14) Zhang, J.; Luo, N.; Wan, J.; Xia, G.; Yu, J.; He, J.; Zhang, J. Directly Converting Agricultural Straw into All-Biomass Nanocomposite Films Reinforced with Additional in Situ-Retained Cellulose Nanocrystals. *ACS Sustainable Chem. Eng.* **2017**, *5*, 5127−5133.

(15) Li, J. Y.; Zhang, X. C.; Zhang, J. M.; Mi, Q. Y.; Jia, F. W.; Wu, J.; Yu, J.; Zhang, J. Direct and complete utilization of agricultural

straw to fabricate all-biomass films with high-strength, high-haze and UV-shielding properties. *Carbohydr. Polym.* **2019**, *223*, No. 115057.
(16) Wang, S.; Peng, X.; Zhong, L.; Jing, S.; Cao, X.; Lu, F.; Sun, R. Choline chloride/urea as an effective plasticizer for production of cellulose films. *Carbohydr. Polym.* **2015**, *117*, 133−139.
(17) Song, J.; Chen, C.; Zhu, S.; Zhu, M.; Dai, J.; Ray, U.; Li, Y.; Kuang, Y.; Li, Y.; Quispe, N.; et al. Processing bulk natural wood into a high-performance structural material. *Nature* **2018**, *554*, 224−228.
(18) Chen, C.; Li, Z.; Mi, R.; Dai, J.; Xie, H.; Pei, Y.; Li, J.; Qiao, H.; Tang, H.; Yang, B.; Hu, L. Rapid Processing of Whole Bamboo with Exposed, Aligned Nanofibrils toward a High-Performance Structural Material. *ACS Nano* **2020**, *14*, 5194−5202.
(19) Guan, Q. F.; Yang, H. B.; Han, Z. M.; Ling, Z. C.; Yu, S. H. An all-natural bioinspired structural material for plastic replacement. *Nat. Commun.* **2020**, *11*, No. 5401.
(20) Soykeabkaew, N.; Sian, C.; Gea, S.; Nishino, T.; Peijs, T. All-cellulose nanocomposites by surface selective dissolution of bacterial cellulose. *Cellulose* **2009**, *16*, 435−444.
(21) Zhang, F.; Lan, X.; Peng, H.; Hu, X.; Zhao, Q. A "Trojan Horse" Camouflage Strategy for High-Performance Cellulose Paper and Separators. *Adv. Funct. Mater.* **2020**, *30*, No. 2002169.
(22) Chen, F.; Xiang, W.; Sawada, D.; Bai, L.; Hummel, M.; Sixta, H.; Budtova, T. Exploring Large Ductility in Cellulose Nanopaper Combining High Toughness and Strength. *ACS Nano* **2020**, *14*, 11150−11159.
(23) Zhao, D.; Huang, J.; Zhong, Y.; Li, K.; Zhang, L.; Cai, J. High-Strength and High-Toughness Double-Cross-Linked Cellulose Hydrogels: A New Strategy Using Sequential Chemical and Physical Cross-Linking. *Adv. Funct. Mater.* **2016**, *26*, 6279−6287.
(24) Ye, D.; Lei, X.; Li, T.; Cheng, Q.; Chang, C.; Hu, L.; Zhang, L. Ultrahigh Tough, Super Clear, and Highly Anisotropic Nanofiber-Structured Regenerated Cellulose Films. *ACS Nano* **2019**, *13*, 4843−4853.
(25) Hu, L.; Zhong, Y.; Wu, S.; Wei, P.; Huang, J.; Xu, D.; Zhang, L.; Ye, Q.; Cai, J. Biocompatible and biodegradable super-toughness regenerated cellulose via water molecule-assisted molding. *Chem. Eng. J.* **2021**, *417*, No. 129229.
(26) Diao, H.; Song, G.; Wu, J.; Zheng, X.; Zhang, J. Stretch-Induced Crystallization of Cellulose Spun from Ionic Liquid Solution. *Biomacromolecules* **2022**, *23*, 2264−2271.
(27) Wen, X.; Su, Y.; Liu, G.; Li, S.; Müller, A. J.; Kumar, S. K.; Wang, D. Direct Relationship between Dispersion and Crystallization Behavior in Poly(ethylene oxide)/Poly(ethylene glycol)-g-Silica Nanocomposites. *Macromolecules* **2021**, *54*, 1870−1880.
(28) Swatloski, R. P.; Spear, S. K.; Holbrey, J. D.; Rogers, R. D. Dissolution of Cellose with Ionic Liquids. *J. Am. Chem. Soc.* **2002**, *124*, 4974−4975.
(29) Xia, Z.; Li, J.; Zhang, J.; Zhang, X.; Zheng, X.; Zhang, J. Processing and valorization of cellulose, lignin and lignocellulose using ionic liquids. *J. Bioresour. Bioprod.* **2020**, *5*, 79−95.
(30) Zhang, J.; Wu, J.; Yu, J.; Zhang, X.; He, J.; Zhang, J. Application of ionic liquids for dissolving cellulose and fabricating cellulose-based materials: state of the art and future trends. *Mater. Chem. Front.* **2017**, *1*, 1273−1290.
(31) Liu, X.; Pang, J.; Zhang, X.; Wu, Y.; Sun, R. Regenerated cellulose film with enhanced tensile strength prepared with ionic liquid 1-ethyl-3-methylimidazolium acetate (EMIMAc). *Cellulose* **2013**, *20*, 1391−1399.
(32) Li, T.; Zhai, Y.; He, S.; Gan, W.; Wei, Z.; Heidarinejad, M.; Dalgo, D.; Mi, R.; Zhao, X.; Song, J.; et al. A radiative cooling structural material. *Science* **2019**, *364*, 760−763.
(33) Khakalo, A.; Tanaka, A.; Korpela, A.; Orelma, H. Delignification and Ionic Liquid Treatment of Wood toward Multifunctional High-Performance Structural Materials. *ACS Appl. Mater. Interfaces* **2020**, *12*, 23532−23542.
(34) Khakalo, A.; Tanaka, A.; Korpela, A.; Hauru, L. K. J.; Orelma, H. All-Wood Composite Material by Partial Fiber Surface Dissolution with an Ionic Liquid. *ACS Sustainable Chem. Eng.* **2019**, *7*, 3195−3202.
(35) Reyes, G.; Borghei, M.; King, A. W. T.; Lahti, J.; Rojas, O. J. Solvent Welding and Imprinting Cellulose Nanofiber Films Using Ionic Liquids. *Biomacromolecules* **2019**, *20*, 502−514.
(36) Zhang, D.; Li, G.; Liu, Y.; Hou, G.; Cui, J.; Xie, H.; Zhang, S.; Sun, Z.; Fang, Z. Favorable combination of foldability and toughness of transparent cellulose nanofibril films by a PET fiber-reinforced strategy. *Int. J. Biol. Macromol.* **2020**, *164*, 3268−3274.
(37) Hosoda, N.; Tsujimoto, T.; Uyama, H. Green Composite of Poly(3-hydroxybutyrate-co-3-hydroxyhexanoate) Reinforced with Porous Cellulose. *ACS Sustainable Chem. Eng.* **2014**, *2*, 248−253.
(38) Zhou, J.; Fang, Z.; Cui, J.; Zhang, X.; Qian, Y.; Liu, W.; Yang, D.; Qiu, X. Wood-inspired strategy to toughen transparent cellulose nanofibril films. *Carbohydr. Polym.* **2021**, *259*, No. 117759.
(39) Liu, G.-C.; He, Y.-S.; Zeng, J.-B.; Li, Q.-T.; Wang, Y.-Z. Fully Biobased and Supertough Polylactide-Based Thermoplastic Vulcanizates Fabricated by Peroxide-Induced Dynamic Vulcanization and Interfacial Compatibilization. *Biomacromolecules* **2014**, *15*, 4260−4271.
(40) Zhang, J.; Li, F.; Liu, T.; Li, Y.; Li, J.; Gao, Q. Tough and strong biomimetic soy protein films with excellent UV-shielding performance. *Composites, Part B* **2021**, *226*, No. 109379.
(41) Zhao, X.; Wu, H.; Guo, B.; Dong, R.; Qiu, Y.; Ma, P. X. Antibacterial anti-oxidant electroactive injectable hydrogel as self-healing wound dressing with hemostasis and adhesiveness for cutaneous wound healing. *Biomaterials* **2017**, *122*, 34−47.
(42) Ghosh, M.; Halperin-Sternfeld, M.; Grinberg, I.; Adler-Abramovich, L. Injectable Alginate-Peptide Composite Hydrogel as a Scaffold for Bone Tissue Regeneration. *Nanomaterials* **2019**, *9*, No. 497.
(43) Yuk, H.; Lu, B.; Zhao, X. Hydrogel bioelectronics. *Chem. Soc. Rev.* **2019**, *48*, 1642−1667.
(44) Wallin, T. J.; Pikul, J.; Shepherd, R. F. 3D printing of soft robotic systems. *Nat. Rev. Mater.* **2018**, *3*, 84−100.
(45) Xu, D.; Huang, J.; Zhao, D.; Ding, B.; Zhang, L.; Cai, J. High-Flexibility, High-Toughness Double-Cross-Linked Chitin Hydrogels by Sequential Chemical and Physical Cross-Linkings. *Adv. Mater.* **2016**, *28*, 5844−5849.
(46) Nian, G.; Kim, J.; Bao, X.; Suo, Z. Making Highly Elastic and Tough Hydrogels from Doughs. *Adv. Mater.* **2022**, *34*, No. e2206577.
(47) Dodda, J. M.; Azar, M. G.; Bělský, P.; Šlouf, M.; Brož, A.; Bačáková, L.; Kadlec, J.; Remiš, T. Biocompatible hydrogels based on chitosan, cellulose/starch, PVA and PEDOT:PSS with high flexibility and high mechanical strength. *Cellulose* **2022**, *29*, 6697−6717.
(48) Huang, K.; Xu, H.; Chen, C.; Shi, F.; Wang, F.; Li, J.; Hu, S. A novel dual crosslinked polysaccharide hydrogel with self-healing and stretchable properties. *Polym. Chem.* **2021**, *12*, 6134−6144.
(49) Kim, H. S.; Lee, K. Y. Stretchable and self-healable hyaluronate-based hydrogels for three-dimensional bioprinting. *Carbohydr. Polym.* **2022**, *295*, No. 119846.
(50) Xue, X.; Song, G.; Chang, C. Tough all-polysaccharide hydrogels with uniaxially/planarly oriented structure. *Carbohydr. Polym.* **2022**, *288*, No. 119376.
(51) Wang, Q.; Pan, X.; Guo, J.; Huang, L.; Chen, L.; Ma, X.; Cao, S.; Ni, Y. Lignin and cellulose derivatives-induced hydrogel with asymmetrical adhesion, strength, and electriferous properties for wearable bioelectrodes and self-powered sensors. *Chem. Eng. J.* **2021**, *414*, No. 128903.
(52) Zhao, D.; Zhu, Y.; Cheng, W.; Xu, G.; Wang, Q.; Liu, S.; Li, J.; Chen, C.; Yu, H.; Hu, L. A Dynamic Gel with Reversible and Tunable Topological Networks and Performances. *Matter* **2020**, *2*, 390−403.
(53) Yeo, J. C. C.; Muiruri, J. K.; Koh, J. J.; Thitsartarn, W.; Zhang, X.; Kong, J.; Lin, T. T.; Li, Z.; He, C. Bend, Twist, and Turn: First Bendable and Malleable Toughened PLA Green Composites. *Adv. Funct. Mater.* **2020**, *30*, No. 2001565.

https://doi.org/10.1021/acssuschemeng.3c02038
ACS Sustainable Chem. Eng. 2023, 11, 9153−9162